J. Membrane Biol. 141, 123–138 (1994)

The Journal of
Membrane
Biology

Potassium Currents in Cultured Rabbit Retinal Pigment Epithelial Cells

Q. Tao[1], P.E. Rafuse[2], M.E.M. Kelly[1]

[1]Department of Pharmacology, Tupper Medical Building, Dalhousie University, Halifax, Nova Scotia, Canada B3H 4H7
[2]Department of Ophthalmology, Dalhousie University, Halifax, Nova Scotia, Canada

Received: 13 December 1993/Revised: 11 April 1994

Abstract. Membrane potential and ionic currents were studied in cultured rabbit retinal pigment epithelial (RPE) cells using whole-cell patch clamp and perforated-patch recording techniques. RPE cells exhibited both outward and inward voltage-dependent currents and had a mean membrane capacitance of 26 ± 12 pF (SD, $n = 92$). The resting membrane potential averaged −31 ± 15 mV ($n = 37$), but it was as high as −60 mV in some cells. When K^+ was the principal cation in the recording electrode, depolarization-activated outward currents were apparent in 91% of cells studied. Tail current analysis revealed that the outward currents were primarily K^+ selective. The most frequently observed outward K^+ current was a voltage- and time-dependent outward current (I_K) which resembled the delayed rectifier K^+ current described in other cells. I_K was blocked by tetraethylammonium ions (TEA) and barium (Ba^{2+}) and reduced by 4-aminopyridine (4-AP). In a few cells (3–4%), depolarization to −50 mV or more negative potentials evoked an outwardly rectifying K^+ current (I_{Kt}) which showed more rapid inactivation at depolarized potentials. Inwardly rectifying K^+ current (I_{KI}) was also present in 41% of cells. I_{KI} was blocked by extracellular Ba^{2+} or Cs^+ and exhibited time-dependent decay, due to Na^+ blockade, at negative potentials. We conclude that cultured rabbit RPE cells exhibit at least three voltage-dependent K^+ currents. The K^+ conductances reported here may provide conductive pathways important in maintaining ion and fluid homeostasis in the subretinal space.

Key words: Voltage-dependent K^+ currents — Retinal pigment epithelial cells — Patch clamp

Correspondence to: M.E.M. Kelly

Introduction

The retinal pigment epithelium (RPE) is a single layer of specialized epithelial cells situated between the retinal photoreceptors and the choriocapillaris. The apical and basal membranes of the vertebrate RPE are coupled by tight junctions between the cells, with the apical membrane directly apposed to the photoreceptors (Zinn & Benjamin-Henkind, 1979). The RPE carries out a myriad of functions to maintain the viability of the outer neural retina and the photoreceptors (Steinberg & Miller, 1979; Zinn & Benjamin-Henkind, 1979). The functions of the RPE include transport of nutrients and cofactors as well as regulation of ion and fluid homeostasis in the subretinal space (Steinberg & Miller, 1979; Immel & Steinberg, 1986; La Cour, Lund-Andersen & Zeuthen, 1986). The capacity of the RPE to remove fluid from the subretinal space is thought to be a major factor contributing to retinal adhesion (Bird, 1989; Marmor, 1989; Zauberman, 1979).

The ion transport mechanisms of the RPE have now been studied in a number of different vertebrate preparations (Miller & Steinberg, 1982 (frog); Joseph & Miller, 1991 (bovine); Quinn & Miller, 1992 (human)). Many of these studies have been directed towards characterization of epithelial K^+ fluxes, since activation of the photoreceptors following light onset results in changes in $[K^+]_o$ in the subretinal space and alterations in the K^+ permeabilities of both the apical and basal RPE membranes (Oakley & Green, 1976; Oakley, 1977; Steinberg, Oakley & Neimeyer, 1980). Alterations in $[K^+]_o$ on the retinal side of the RPE have been shown to induce changes in the membrane potential of RPE cells and contribute to the autoregulation of K^+ activity in subretinal space (Oakley, 1977; Immel & Steinberg, 1986; La Cour et al., 1986).

To date, several populations of K^+ channels have been described in RPE cells from a variety of species.

Ionic currents have been investigated at the whole-cell level in freshly dissociated cells derived from both frog and turtle RPE (Hughes & Steinberg, 1990; Fox & Steinberg, 1992). These studies revealed that amphibian and reptilian RPE cells possess both inwardly rectifying and outwardly rectifying voltage-dependent K^+ currents. Single channel recordings from the apical membranes of cultured human RPE cells also have revealed several different populations of K^+-selective channels; however, none of these channels showed any voltage dependence (Fox, Pfeffer & Fain, 1988). More recently, several reports have described whole-cell voltage-dependent Ca^{2+} and K^+ currents in freshly isolated rat RPE cells (Hughes, Botchkin & Steinberg, 1990; Strauß & Weinrich, 1992; Ueda & Steinberg, 1993) and in fresh and cultured primate RPE cells (Strauß, Richard & Weinrich, 1993; Wen, Lui & Steinberg, 1993). These studies revealed that, like amphibian RPE cells, mammalian RPE cells may exhibit several different voltage-dependent K^+ currents, although further comparative studies are required to resolve the functional implications of these different ion channels.

In the present study, we have used whole-cell patch clamp recording methods to investigate the membrane properties and K^+ conductances of cultured rabbit RPE cells. Since the rabbit is a well-established animal model for ocular research, information on the ionic conductances in this species is essential to facilitate interpretation of transport data and extrapolate data between different animal models. We provide both pharmacological and kinetic evidence that rabbit RPE cells in culture express at least three separate K^+ conductances. Two distinct voltage- and time-dependent outwardly rectifying K^+ currents and a voltage-dependent inwardly rectifying K^+ current are described. In addition, we also report that, using standard whole-cell and perforated-patch recording, no inward voltage-dependent Na^+ and Ca^{2+} currents were apparent. Some of this work has been presented in abstract form (Tao, Kelly & Rafuse, 1993).

Materials and Methods

Cell Dissociation and Culture

Eyes were harvested from 5–10-week-old pigmented rabbits. Animals were euthanized with sodium-pentobarbitol (MTC Pharmaceuticals, Cambridge, Ontario), following which the eyes were enucleated and placed in phosphate-buffered saline (PBS). Using aseptic conditions, the globes were divided below the ora serrata and the anterior segment and vitreous were removed. The neural retina was then gently peeled off using forceps and the posterior eye cups incubated in sterile PBS-containing 0.05% EDTA for 40 min at room temperature. Eye-cups were then irrigated with fresh EDTA-free PBS and separated RPE sheets obtained by gentle aspiration. RPE tissue was then triturated through a narrow-bore glass pipette to yield a single cell suspension. Isolated cells were washed and resuspended in Dulbecco's modified Eagle's medium (DMEM) plus 10% fetal calf serum and 0.5% penicillin-streptomycin (all culture reagents from GIBCO BRL, Burlington, Ontario). The cell viability was estimated by exclusion of trypan blue and was generally greater than 90%. Cells were seeded onto coverslips (12 mm diameter) in 35 mm plastic petri dishes and placed in a 37°C incubator with an atmosphere of 5% CO_2/95% O_2. Cells were maintained in primary culture for 2–5 days and identified by morphological criteria (*see* Results) prior to recording.

Superfusion and Solutions

Cells, attached to glass coverslips, were placed in a shallow recording chamber and positioned on the stage of a Nikon inverted microscope. Cells were superfused (1–2 ml/min) with standard physiological solution composed of (in mM): NaCl, 130; KCl, 5; $CaCl_2$, 2.5; $MgSO_4$, 1; Na_2HCO_3, 25; HEPES, 5; glucose, 10. All solutions were continuously bubbled with 5% CO_2/95% O_2; adjusted to pH 7.4 with NaOH. External solutions were gravity-fed into the recording chamber from elevated reservoirs and selected by a series of switches designed to maintain a constant flow. In experiments where pharmacological blockade of ionic currents was studied, test solutions were applied by bath superfusion or by pneumatic pressure ejection (Picospritzer II, General Valve, Fairfield, NJ) from micropipettes (tip diameter 1–2 μm) positioned approximately 50–100 μm from the cell. For those experiments where external K^+ was increased, NaCl was replaced with the equimolar amounts of KCl to a final concentration of 25 or 50 mM K^+. In experiments which investigated the time-dependent decay of the whole-cell inward current at negative potentials, Na^+ was substituted with *N*-methyl-D-glucamine$^+$ ($NMDG^+$). Electrode filling solution for both whole-cell and perforated-patch recordings was composed of (in mM): KCl, 140; $MgCl_2$, 1; HEPES, 20; EGTA, 1; $CaCl_2$, 0.4; ATP (Mg), 1; GTP(Na_2), 0.1; adjusted to pH 7.4 with KOH. Free [Ca^{2+}] was estimated to be ≈100 nM. Solution osmolarities were determined by freezing point depression. External solutions had a final osmolarity of between 330–340 mOsm and the osmolarity of internal solutions was 320 mOsm. The use of a slightly hyperosmotic external solution was found to be effective in eliminating transient changes in ionic conductances, occurring as a result of osmotic changes, during the initial period of time following attainment of whole-cell recording configuration.

When the perforated-patch technique was used, nystatin was dissolved in dimethylsulfoxide (50 mg/ml) and diluted to a final concentration of 0.1 mg/ml in electrode solution. The electrode tips were filled with nystatin-free electrode solution and backfilled with nystatin-containing solution. All chemicals were from Sigma Chemical (St Louis, MO).

Electrophysiological Recording Techniques

We used the whole-cell configuration of the patch clamp recording technique (Hamill et al., 1981) and the nystatin perforated-patch method (Horn & Marty, 1988). Patch electrodes were pulled from borosilicate glass micropipettes with 1.5 mm outside diameter and 1.1 mm inside diameter (Sutter Instruments, Novato, CA) on a two-stage vertical microelectrode puller (Narishige, PP83, Tokyo, Japan). Electrodes had resistances of 2 to 3 MΩ when filled with internal solution and placed in the bath solution. Electrodes were coated with beeswax to reduce capacitance. The bath solution was connected to the reference electrode by a 3 M KCl-2% agar bridge. Offset potentials were nulled using the amplifier circuitry before seals were made on cells. Junction potentials of 1–2 mV, measured between the bath and patch clamp electrodes, were not corrected in the data shown unless noted otherwise. Membrane potential and ionic currents were

recorded with an Axopatch 1D amplifier (Axon Instruments, Foster City, CA). Currents were filtered with a 4-pole low-pass Bessel filter (−3 dB at 1 kHz) and digitized at a sampling frequency of 5 kHz using pCLAMP software (Axon Instruments). Values of current and voltage reported in figures are averages of 10 to 50 points. Current and voltage were displayed on a Gould TA240 chart recorder and stored on computer disk as well as on video tape using a pulse code modulator (Medical Systems, Greenvale, NY). All experiments were conducted at room temperature (21–22°C). Values for cell-capacitance were obtained from the capacitance compensation circuitry on the amplifier or by integration of the uncompensated current transient (obtained using 10 mV voltage commands). Measures of series resistance (R_{access}) were obtained directly from the amplifier and were generally less than 15 MΩ. Eighty percent series resistance compensation was used in most cases. In some cells, current records were corrected for a linear leakage current measured from hyperpolarizing command pulses. Where currents have been leak-substracted this value is stated in the figure legend. Data are presented as mean ± SD.

Results

Cell Identification

Using phase-contrast optics, freshly isolated RPE cells were identified by their polygonal shape and the presence of melanin granules (Fig. 1*A*). Previously, we reported that pigmented rabbit RPE cells in culture exhibit staining for cytokeratins, the intermediate filament proteins characteristic of many epithelial cells (Tao et al., 1993). Within 1–2 days after plating, RPE cells attach to the substrate. For electrophysiological recordings, cells were generally used at 2–5 days in culture. Two typical cells from which recordings were made are shown in Fig. 1*B* and *C*. In Fig. 1*B*, the apical portion of the cell is readily distinguished by the presence of pigment granules as well as cellular processes. No recordings were made from cells that were devoid of pigment.

Whole-Cell Currents and Membrane Properties

Under voltage clamp, RPE cells exhibited both outward and inward current in response to depolarizing and hyperpolarizing voltage commands. Figure 2 shows whole-cell currents recorded from two different RPE cells with 140 mM KCl in the pipette. Cells were held at −60 mV and stepped from −120 to +60 mV in 20 mV increments. In Fig. 2*A*, the cell shows little current in response to hyperpolarizing voltage commands. However, at positive potentials outward current is apparent. The *I-V* relationship for this cell, measured at 500 msec, is shown in Fig. 2*B* with outwardly rectifying current activating at −40 mV. Figure 2*C* shows whole-cell currents recorded from another cell. This cell exhibits steady inward current at hyperpolarized potentials as well as outward current at depolarized potentials. The *I-V* relation in Fig. 2*D* shows that inwardly rectifying current is apparent between −120 to −70 mV, with outwardly rectifying current activating around −40 mV.

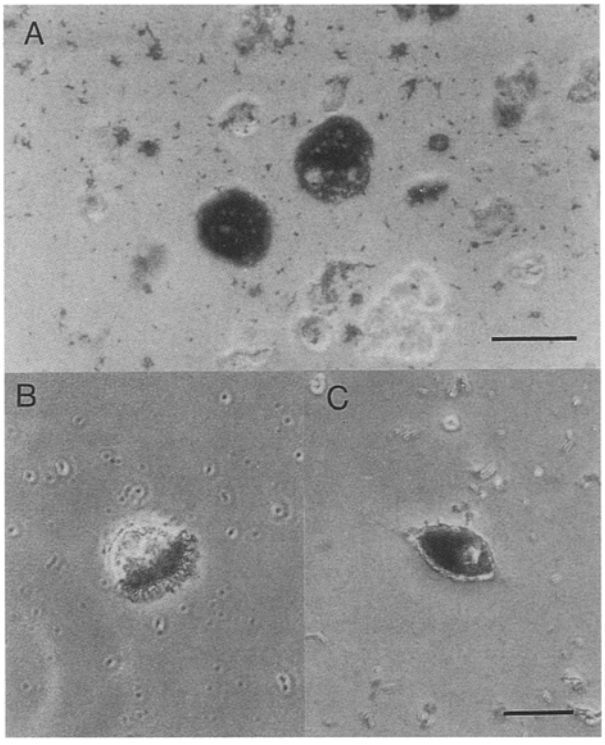

Fig. 1. Identification of rabbit RPE cells in culture. (*A*) Phase-contrast photomicrograph of freshly isolated rabbit RPE cells. (*B* and *C*) Representative RPE cells used for recording. Cells have been growing for three days in primary culture. Scale bar equals 20 μm in *A*, and 10 μm for *B* and *C*.

The two voltage-dependent currents described above were the predominant currents observed in cultured rabbit RPE cells. Of a total of 92 RPE cells recorded from using standard whole-cell recording conditions (140 mM KCl in the pipette, NaCl external solution), 91% of RPE cells exhibited outwardly rectifying current, 41% inwardly rectifying current and 37% of cells exhibited both inward and outward current. The average cell capacitance measured was 26 ± 13 pF (n = 91) and the resting membrane potential (RMP) measured in current clamp in 37 cells averaged −31 ± 15 mV, but was as high as −60 mV in some cells. Similar average values for RMP were also reported for dissociated frog and turtle RPE cells (Hughes & Steinberg, 1990; Fox & Steinberg, 1992) and for human RPE cells in culture (Fox et al., 1988).

Outward Current is K^+ Selective

The ionic selectivity of the outward current was investigated in different K^+-containing solutions by examining time- and voltage-dependent current relaxations

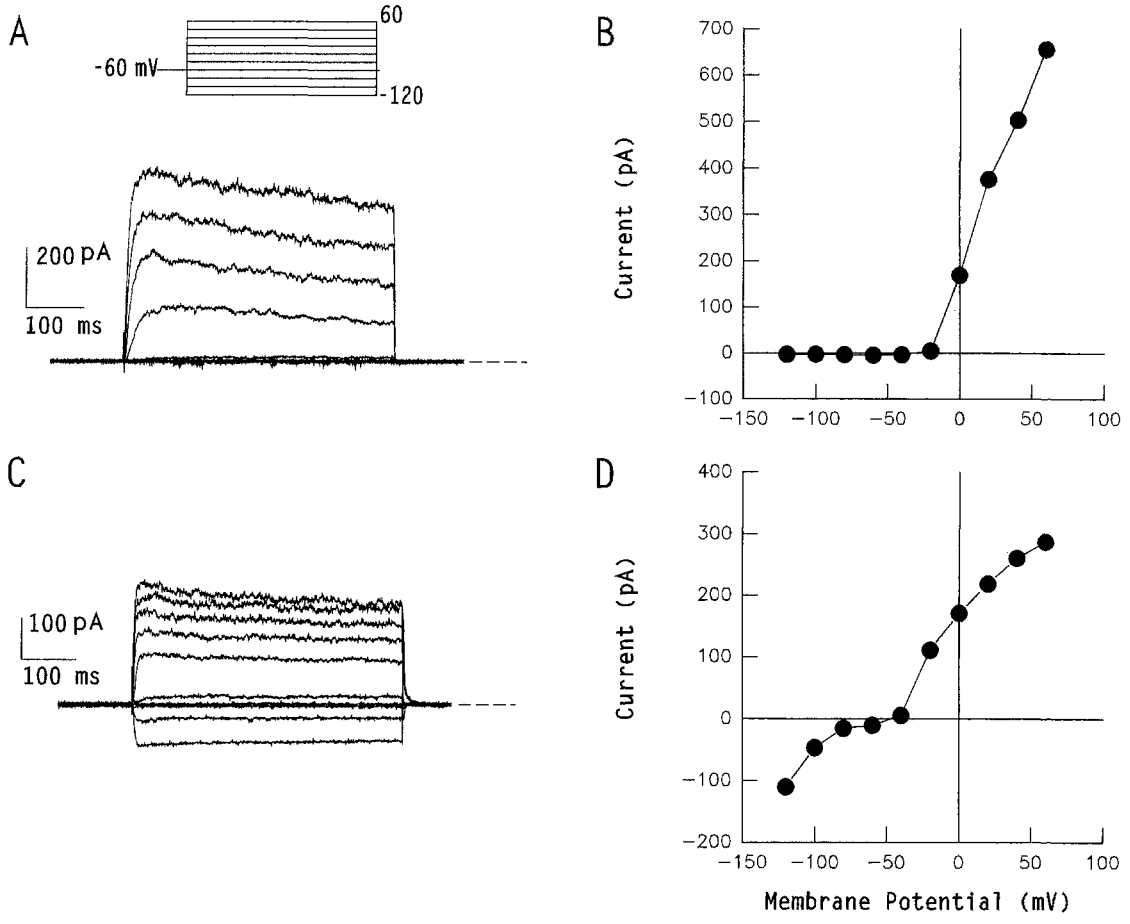

Fig. 2. Voltage-dependent K^+ currents in rabbit RPE cells. Whole-cell currents recorded from RPE cells in standard NaCl external Ringer with 140 mM KCl in the pipette. The voltage-clamp protocol is shown at the top center. (*A*) Currents elicited in an RPE cell by a group of voltage commands from −120 to +60 mV, from a holding potential (V_H) of −60 mV. Outward current is activated at potentials of −40 mV and more positive, with little current apparent at more negative potentials. A linear leak of 1.7 GΩ was subtracted from the current traces shown. (*B*) Current-voltage (*I-V*) plot for the cell shown in *A*, measured 50 msec after the start of the voltage command. (*C*) Currents recorded in another RPE cell using the same voltage clamp protocol as in *A*. At hyperpolarized potentials, steady inward current is seen with outward current activating at more positive potentials. Currents were subtracted for a linear leak of 2 GΩ. (*D*) The *I-V* plot for the cell in *C* shows inwardly rectifying current between −50 to −120 mV and outwardly rectifying current activating at −40 mV. Capacitance of the cells shown in *A* and *C* was 24 and 57 pF, respectively. Dashed lines indicate the zero current potential in this and subsequent figures.

(tail currents), following activation of outward current by a test voltage step to +20 mV (Fig. 3*A*). Tail currents recorded in standard 5 mM $[K^+]_o$, 25mM $[K^+]_o$, and 50 mM $[K^+]_o$ are shown in Fig. 3*B*. In 5 mM $[K^+]_o$ tail currents reversed direction at -72 ± 6 mV ($n = 4$), which approaches the value of −85 mV calculated for the K^+ equilibrium potential (E_K) under our recording conditions. When $[K^+]_o$ was increased to 25 and 50 mM, respectively, the reversal potential of the tails shifted to more positive values. In 25 mM $[K^+]_o$ tail currents reversed at -41 ± 1 mV and in 50 mM $[K^+]_o$ tail currents reversed at -23 ± 6 mV. A least squares fit to the data is shown in Fig. 3*C*. The fitted line has a slope of 50 mV per 10-fold change of $[K^+]_o$, which is close to the predicted value of 58 mV per 10-fold change in $[K^+]_o$, and suggests that the outward current is largely selective for K^+ ions. Further analysis of the tail currents revealed that they were best approximated by single exponentials. The time constants for decay of the tail currents were voltage dependent and this dependence was similar in 5, 25 and 50 mM $[K^+]_o$ (*not shown*).

Voltage Dependence and Kinetics of the Outward Current

Outwardly rectifying K^+ current was the predominant current recorded in rabbit RPE cells under standard whole-cell recording conditions with KCl in the recording pipette (84/92 cells). Examination of the activation of the outward K^+ current was carried out using small voltage increments from a prepulse potential at −100 mV. Figure 4*A* illustrates a typical family of outward currents evoked by 1 sec voltage pulses, ranging from

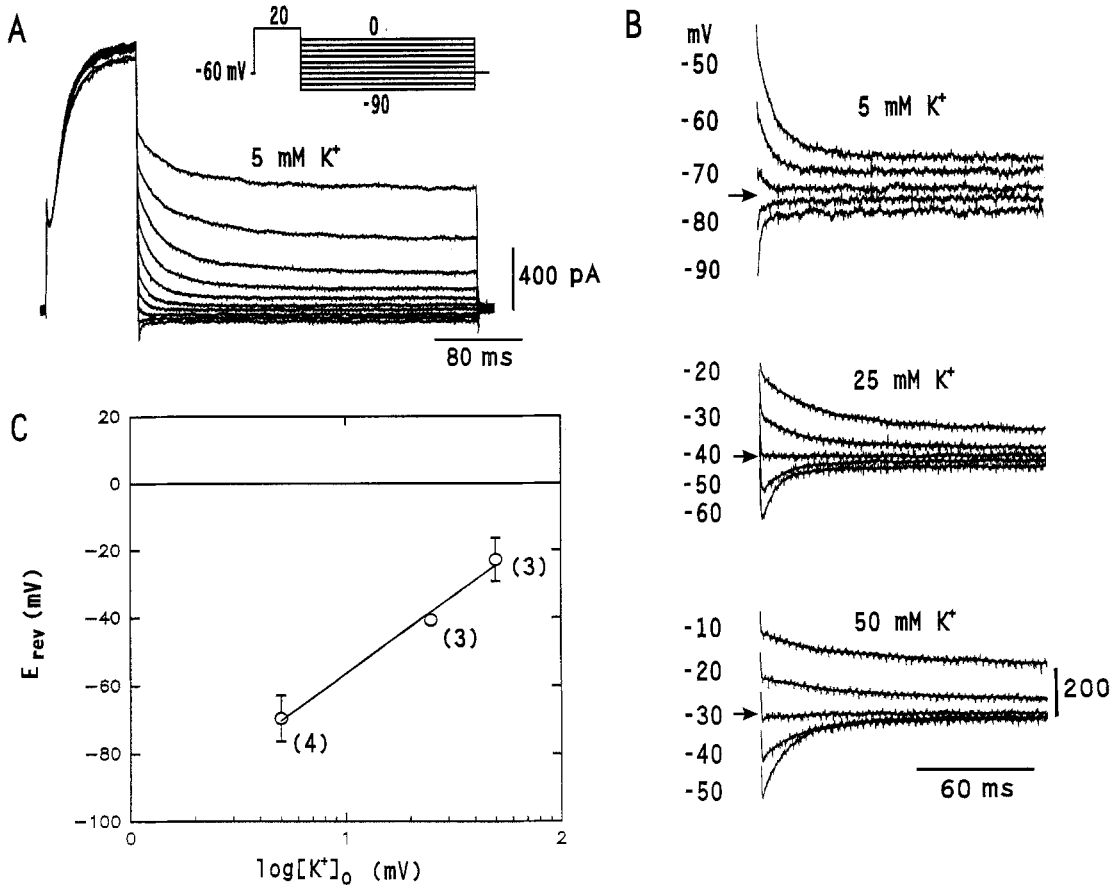

Fig. 3. Outward currents in rabbit RPE cells are carried by K^+ ions. (*A*) Tail currents recorded at various potentials in standard 5 mM K^+ Ringer following a preceding pulse to +20 mV to activate outward current. The voltage-clamp protocol is shown above the traces. (*B*) Expanded view of tail currents recorded from the same cell following sequential superfusion of 5, 25 and 50 mM $[K^+]_o$. Tail currents reversed near −75, −40 and −28 mV, respectively. (*C*) Plot of the reversal potential of the tail currents *vs* extracellular $[K^+]$ for 3–4 cells. The slope of the line fitted by least squares has a slope of 50 mV per 10-fold change in extracellular $[K^+]$. Error bars indicate SD for this and subsequent figures. Capacitance of the cell shown in *A* and *B* was 27 pF.

−50 to +60 mV in 10 mV increments. Outward K^+ current in this cell begins to activate at around −40 mV, with the activation rate increasing at more positive potentials. Since tail current analysis demonstrated that the outward current is carried by K^+, chord conductance can be calculated using the following relationship:

$$I_p = g(V - E_K) \quad (1)$$

where I_p is the peak outward current at membrane potential V, g is the corresponding conductance and E_K is −85 mV, calculated under our recording conditions. The calculated peak conductance for each test pulse was then normalized with respect to the peak conductance evoked by a depolarizing step to +60 mV. Figure 4*B* shows the mean conductance for three cells plotted *vs.* the command potential. The voltage dependence of activation is well described by a Boltzmann equation:

$$g/g_{max} = \{1 + \exp[(V_n - V)/k_n)\}^{-1} \quad (2)$$

where g/g_{max} is the normalized conductance, V is the membrane potential during the test pulse, V_n is the voltage at which the conductance g is half-maximal and k_n gives the steepness of the voltage dependence. The conductance increased sigmoidally with a threshold for activation at −30 mV and saturated at approximately +60 mV. The maximal conductance (g_{max}) averaged 5.4 ± 1.7 nS (n = 3), V_n was +15 mV and k_n was +13 mV.

The amplitude of the outward K^+ current exhibited a slow decline during maintained depolarizing pulses. Figure 5*A* shows outward currents elicited by 1 sec voltage pulses from a prepulse potential of −100 mV to various potentials ranging from 0 to +60 mV. The time course of the decay of the outward current was well described by a single exponential, as shown by the

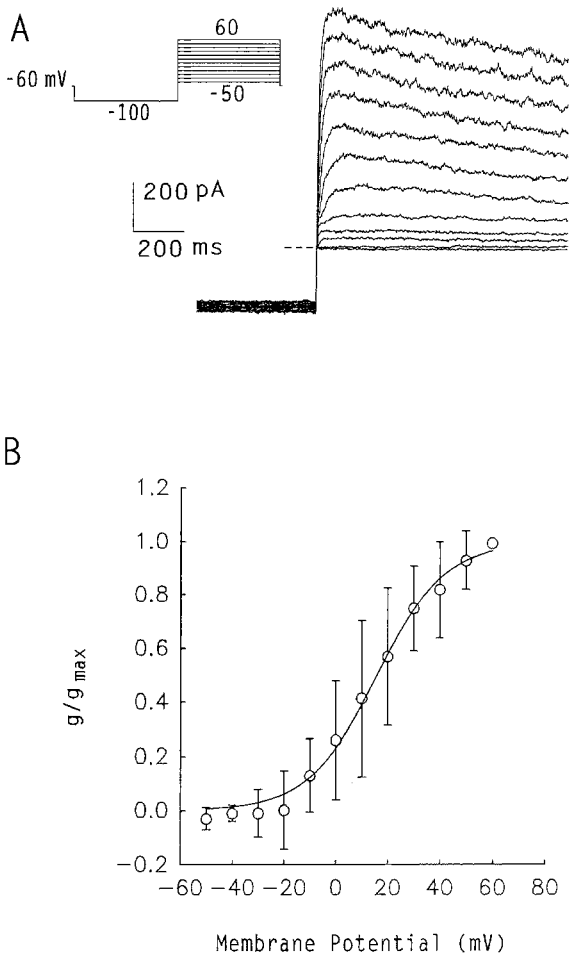

Fig. 4. Activation of outward K^+ current in rabbit RPE cells. (*A*) Outward current was evoked by voltage steps from −50 to +60 mV in 10 mV increments, from a prepulse voltage of −100 mV. Voltage protocol is shown at the top of *A*. Outward current activates around −40 mV and activation becomes more rapid with increasing depolarization. Current traces were leak-subtracted for a linear leak of 1.6 GΩ. (*B*) Outward K^+ conductance (expressed as a fraction of the maximum conductance at +60 mV) plotted as a function of the membrane potential. Conductance values were calculated from the peak current values using Eq. (1) given in the text. Each point represents the mean value from four cells. The smooth line was fitted using the Boltzmann Eq. (2). Capacitance for the cell in *A* was 41 pF.

smooth curve overlying the traces, which displayed little voltage dependence between 0 to +60 mV. The time constant for decay of the outward current at positive potentials ranged from 1.0–2.2 sec, with a mean value of 1.74 ± 0.67 sec (n = 4) at +60 mV (Fig. 5*B*). We also examined the steady-state inactivation of the outward current by applying 10 sec prepulses prior to test voltage steps to + 10 mV for 1 sec (Fig. 5*C*). At prepulse potentials negative to −40 mV, the amplitude of the current at +10 mV is little changed; however, outward current decreased with more positive prepulses. Figure 5*D* shows the peak outward current from the cell in Fig. 5*C* plotted as a function of the prepulse potential. Peak current values were normalized with respect to the peak current evoked from the most hyperpolarizing prepulse. The smooth curve is the nonlinear least squares fit of the data to a Boltzmann function:

$$I/I_{max} = \{1 + \exp[(V - V_n)/k_n]\}^{-1} \quad (3)$$

where I/I_{max} is the normalized current, V is the membrane potential during the test pulse, V_n is the voltage at which I is half-maximal and k_n is the slope factor. In the two cells shown in Fig. 5*D*, steady-state inactivation of the outward K^+ current was half-maximal at −18 mV, with a slope factor of −5.4 mV.

Effects of K^+ Channel Blockers on the Outward K^+ Current

We examined the sensitivity of the outwardly rectifying K^+ current to K^+ channel blockers. Superfusing of 1 mM TEA, which blocks the delayed rectifier K^+ channels in a number of different cell types (Stanfield, 1983), partially blocked the outward current in rabbit RPE cells (Fig. 6*A*). In six cells tested, TEA (1 mM) reversibly reduced the outward current at 0 mV by 60 ± 33% and by 58 ± 16% at +60 mV. Figure 6*B* shows the *I-V* plot for the cell shown in Fig. 6*A*, in control Ringer and during superfusion with 1 mM TEA. The TEA difference current, obtained by digital subtraction of currents measured in control Ringer and following superfusion of TEA, is also shown. TEA reduced the outward current at all potentials where it was activated. In three other cells, 10 mM TEA reduced the outward current at 0 and +60 mV by 86 ± 10 and 89 ± 8%, respectively. The outward K^+ current was also partially blocked by low concentrations of extracellular 4-aminopyridine (Fig. 6*C*); 4-AP, at concentrations of 100 μM reduced the outward current at 0 and +60 mV by approximately 48 ± 30% and 37 ± 14% (n = 3). Increasing the concentration of 4-AP to 1 mM, resulted in a further reduction of the outward current by 70 ± 13% at 0 mV and 40 ± 19% (n = 4) at +60 mV. We also tested the sensitivity of the outward K^+ current to barium, which blocks delayed rectifier K^+ channels on a one-to-one stoichiometric basis (Armstrong & Taylor, 1980). In rabbit RPE cells, 1 mM barium reduced the outward current at 0 and +60 mV by 84 ± 16% and 57 ± 3% (n = 6) (Fig. 6*D*).

Fast-Inactivating Outward K^+ Current

In 3 of the 92 rabbit RPE cells investigated, the outward current had an initial fast inactivation followed by a slower inactivation phase at depolarized potentials. Figure 7*A* shows currents recorded from a cell with fast-inactivating outward current. The cell was held at −60 mV and stepped from −120 to +100 mV in 20 mV in-

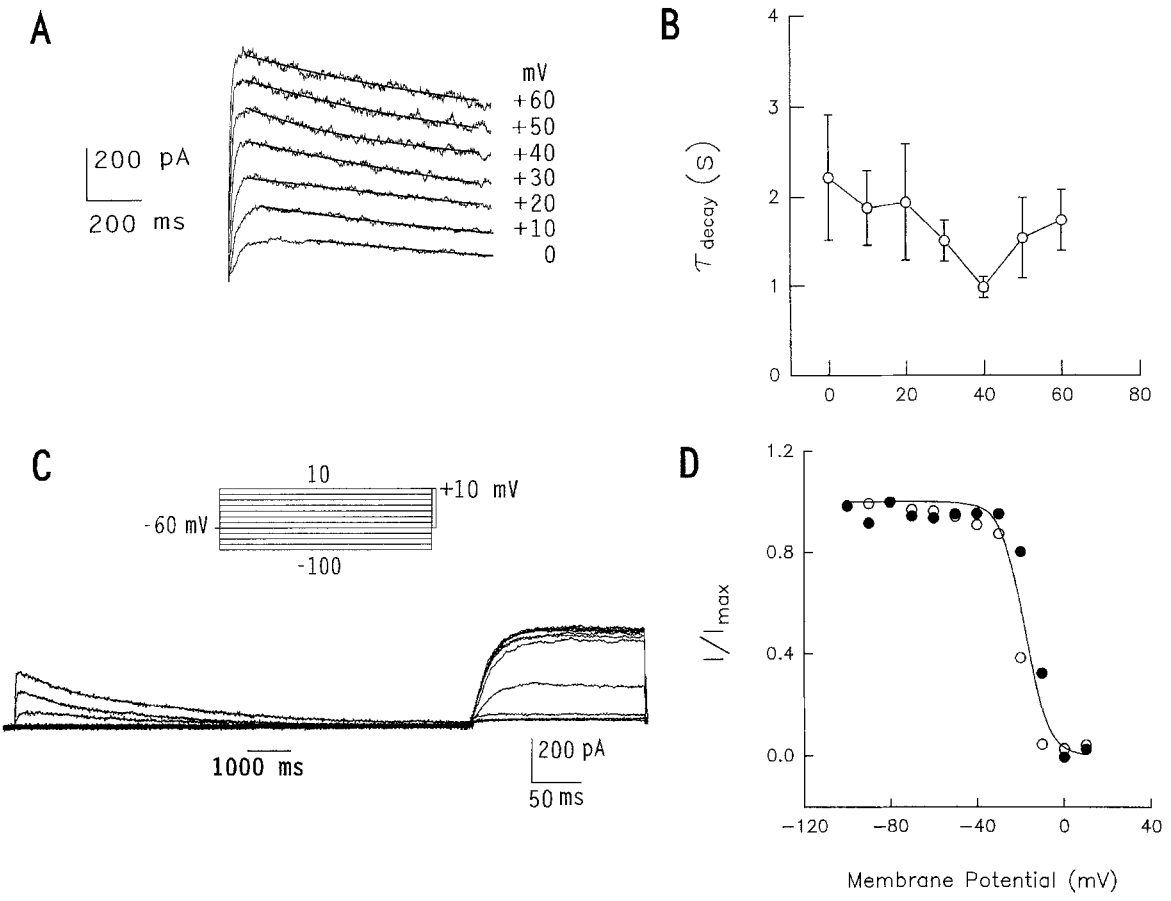

Fig. 5. Inactivation of outward K^+ currents. (*A*) Outward currents recorded from an RPE cell superfused with standard NaCl Ringer with 140 mM KCl in the pipette. The cell was held at −100 mV for 1 sec and then the membrane potential was stepped to potentials ranging from 0 to +60 mV in 10 mV increments. The outward current shows a slow time-dependent decline during the voltage clamp step. The smooth curves overlying the traces indicate single exponential fits to the data. (*B*) Voltage dependence of the decay time constant. Each point represents the mean measurement from four cells. (*C*) Steady-state inactivation of the outward K^+ current. The cell was held at −60 mV and then stepped from −100 to +10 mV in 10 mV increments for 10 sec prior to a test pulse to +10 mV. The outward current decreased with prepulse potentials positive to −50 mV. Currents were subtracted for a linear leak of 1.95 GΩ. (*D*) Plot of the peak outward current (*I*), expressed as a fraction of the maximal current (I_{max}) at +10 mV, as a function of the prepulse potentials for the cell in *C* (○) and one other representative cell (●). The smooth curve through the data points is the best fit to a Boltzmann function, given by Eq. (3) in the text.

crements. Outward current activated around −60 mV and peaked between +40 and +80 mV. Figure 7*B* shows the *I-V* plot for the peak and steady-state currents displayed in Fig. 7*A*. Time-dependent inactivation of the outward current was apparent at potentials positive to 0 mV and increased with depolarization, as evidenced by the difference between the peak and steady-state current at depolarized potentials. Inactivation at +40 mV was well described by a single exponential with a time constant of 122 ± 19 msec (n = 3). Figure 7*C* shows the chord conductance plotted as a function of membrane potential for the cell shown in Fig. 7*A*. Since the outward conductance peaked at +40 mV and then declined at more positive potentials, chord conductances measured for potentials of −120 to +40 mV were normalized to the peak maximum conductance at +40 mV. The voltage dependence of the outward K^+ conductance was well described by the Boltzmann equation (Eq. 2) given previously (continuous smooth line). The maximal peak conductance was 9.97 nS, V_n was −33.5 mV and k_n was +9.5 mV.

Since only 3–4% of rabbit RPE cells at 3–5 days culture exhibited fast-inactivating outward K^+ current, extensive pharmacological characterization was not carried out. However, in two cells with fast-inactivating outward current, quinine reversibly blocked the outward current. Figure 8*A* shows current traces recorded at a potential of +60 mV from a cell with fast-inactivating outward current. Application of 1 mM quinine via an application pipette reversibly blocked the outward current at 0 and +60 mV by 97 and 96%, respectively. The quinine difference current, obtained by subtracting current in the presence of quinine from control current at +60 mV, is shown in Fig. 8*B*.

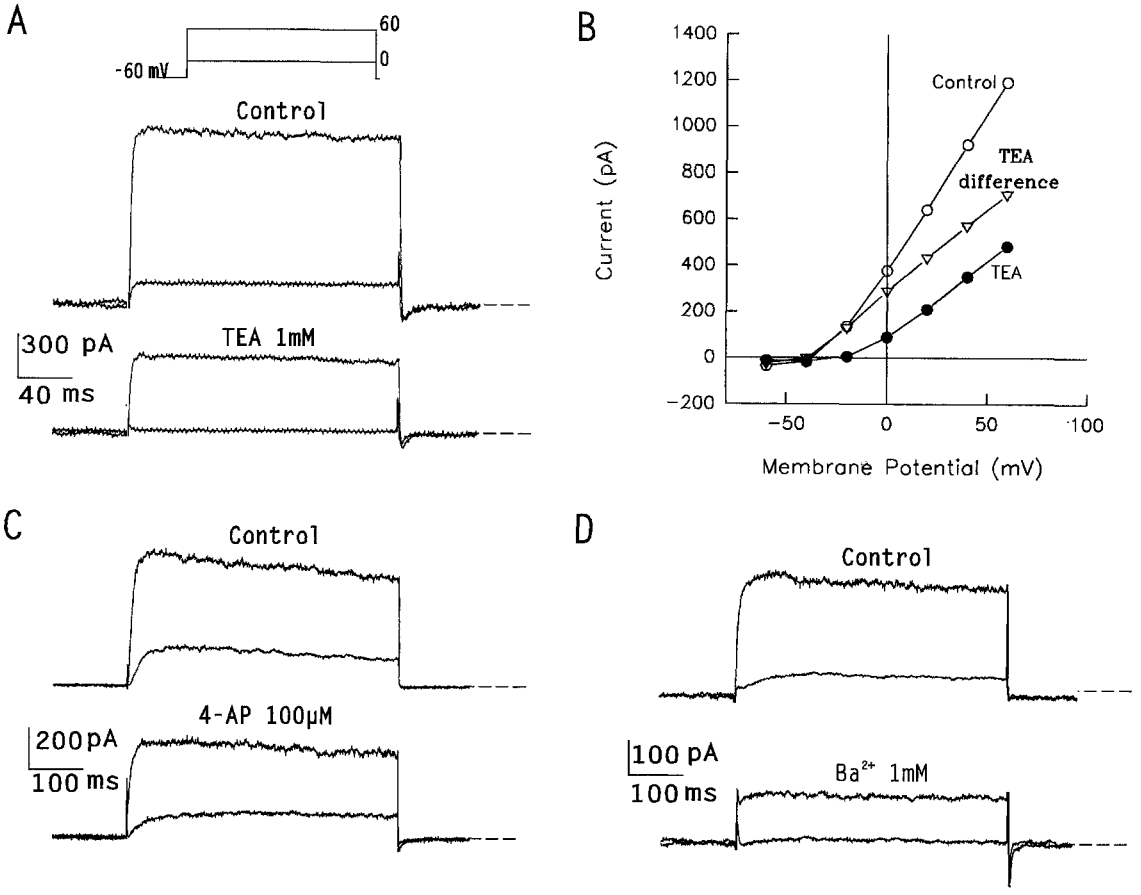

Fig. 6. Pharmacology of the outward K^+ current. (*A*) Outward current evoked by a voltage step from a holding potential of −60 mV to test potentials of 0 and +60 mV for 250 msec. Current traces measured before and during application of 1 mM TEA in the superfusate are shown for comparison. (*B*) *I-V* plot for currents recorded from the cell shown in *A*, measured before (○), and during superfusion with TEA (●). The TEA difference current (▽) is also shown. (*C* and *D*) Outward currents measured at 0 and +60 mV in two other cells before and during application of 100 μM 4-AP (*C*), and 1 mM Ba^{2+} (*D*). Capacitance of the cells shown was 41 pF for the cell in *A* and 22 and 38 pF for the cells in *C* and *D*, respectively.

The Inwardly Rectifying Current in Rabbit RPE Cells Is Selective for K^+

Under voltage clamp, 41% (38/92) of RPE cells exhibited inward current in response to hyperpolarizing voltage commands (Fig. 9). The selectivity of the inwardly rectifying current for potassium ions was investigated by varying the concentration of K^+ in the bathing solution. Figure 9*A* shows inward current recorded in a rabbit RPE cell superfused with 5 mM and subsequently with 50 mM $[K^+]_o$. In 5 mM $[K^+]_o$, inward current is apparent on hyperpolarization of the cell from the holding potential of −60 to −120 mV. When the bathing solution was switched to one containing 50 mM $[K^+]_o$, inward current at −120 mV increased. Figure 9*B* shows the *I-V* relationships for the cell shown in Fig. 9*A*, recorded in standard external solution (5 mM K^+), and then during superfusion with 50 mM $[K^+]_o$. Voltage values for current reversal (V_{REV}) were determined as the potential at which the *I-V* relation intersected the zero current level. Increasing $[K^+]_o$ shifted the reversal potential, and the voltage around which the rectification occurred, positive along the voltage axis. The slope conductance of the *I-V* relationship at negative potentials also increased as $[K^+]_o$ was increased. For the cell shown in Fig. 9*A*, the slope conductance, calculated from the *I-V* relationship in Fig. 9*B*, increased from 5.25 nS in 5 mM external K^+ solution to 19.8 nS in 50 mM external K^+ solution. V_{REV} was dependent on $[K^+]_o$. The straight line in Fig. 9*C* is the least squares best fit of the data measured in 7–12 cells and has a slope of 50 mV per 10-fold change of $[K^+]_o$, suggesting that the inward rectifier in rabbit RPE cells is largely selective for K^+ ions. Further verification that the hyperpolarization-activated inward current is a K^+ current was obtained by examination of time- and voltage-dependent current relaxations following a step to −140 mV to activate inward current and then to more depo-

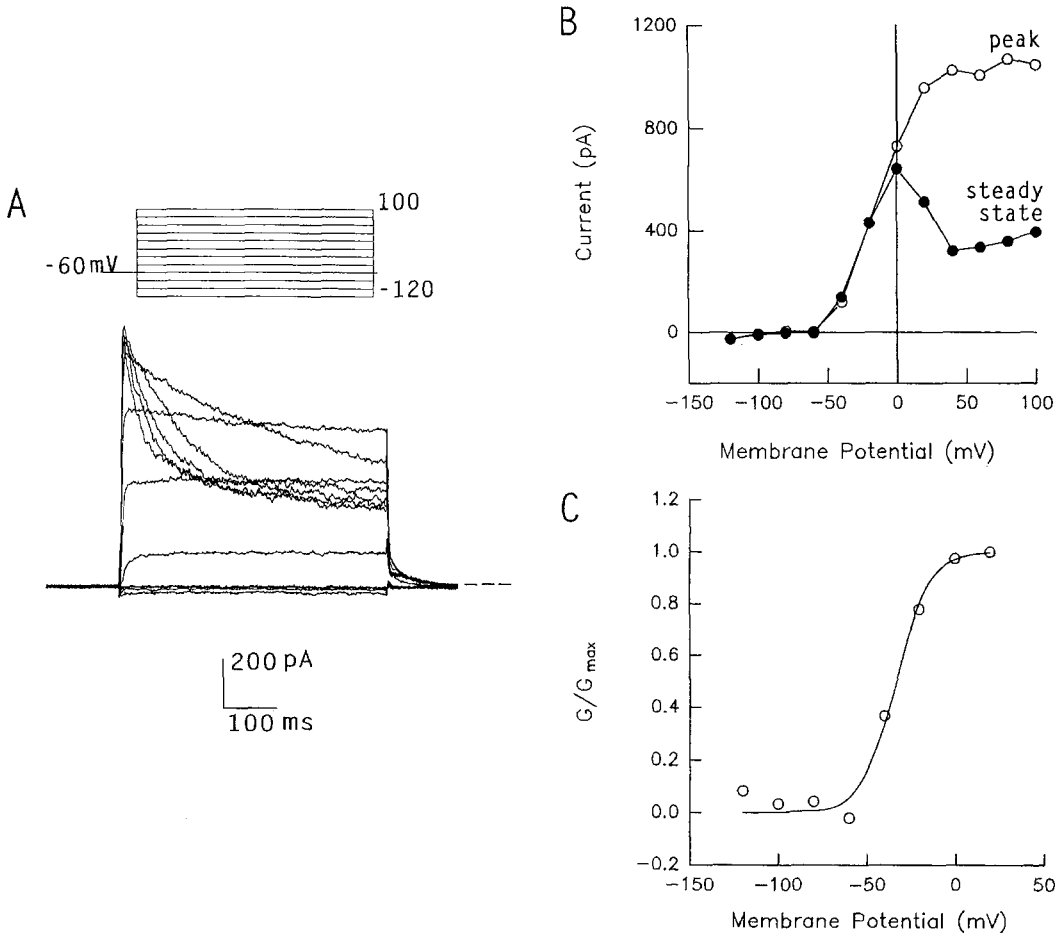

Fig. 7. Voltage dependence of the fast-inactivating outward current. (*A*) The cell was held at −60 mV and stepped to +100 mV in 20 mV increments for 500 msec. (*B*) *I-V* relationship for the currents shown in *A*. Peak outward current was measured at 2 msec (○) and also at 485 msec (●) after the start of the voltage step. (*C*) Conductance, calculated from the peak current using Eq. (1) from the text, expressed as a fraction of the maximum conductance at +40 mV and plotted as a function of the membrane potential during the test pulse. The activation curve was sigmoidally shaped and well described by the Boltzmann Eq. (2) reported in the text (continuous smooth line), with V_n = −33.5 mV and a slope factor of +9.5 mV. Capacitance of the cell was 44 pF.

larized potentials to observe current relaxations (Fig. 9*D*). The reversal potential for "tail" currents was calculated by interpolation between the two nearest points where the current reversed direction. In standard solution, the reversal potential was −82 ± 5 mV (n = 12) which is very close to the K^+ equilibrium potential (−85 mV) calculated under our recording conditions.

Barium and Caesium Block the Inward Rectifier

Both Ba^{2+} and Cs^+ have been demonstrated to block inward rectifier K^+ currents in a number of different cell types (Sakmann & Trube, 1984; Gallin & McKinney, 1988*a*; Adams & Nonner, 1990; Kelly, Dixon & Sim, 1992; Ishikawa & Cook, 1993). Figure 10 shows the effects of externally applied Ba^{2+} and Cs^+ on whole-cell K^+ currents recorded from rabbit RPE cells. The currents shown in Fig. 10*A* were recorded from a cell bathed in standard 5 mM K^+ solution with 140 mM KCl in the recording pipette. At hyperpolarizing potentials an inward current (I_{KI}) is apparent. Following a 30 sec exposure of the cell to external Ba^{2+} (1 mM from an application pipette), inward current is reduced. The peak *I-V* relation for the cell before and after Ba^{2+} is shown in Fig. 10*B*. Ba^{2+} reduced the inward current by 55% at −120 mV. Ba^{2+} also reduced depolarization-activated outward current in this cell. In two other cells tested, superfusion of 1 mM external Ba^{2+} reversibly reduced I_{KI} at −120 mV by 76 and 95%. We also tested the effects of external Cs^+ on the inward rectifier. Figure 10*C* shows representative current traces recorded at negative membrane potentials from another cell bathed in 50 mM K^+ Ringer. Inward current is blocked by 5 mM Cs^+ applied from an application pipette. Figure 10*D* shows the *I-V* relation recorded for the cell in Fig.

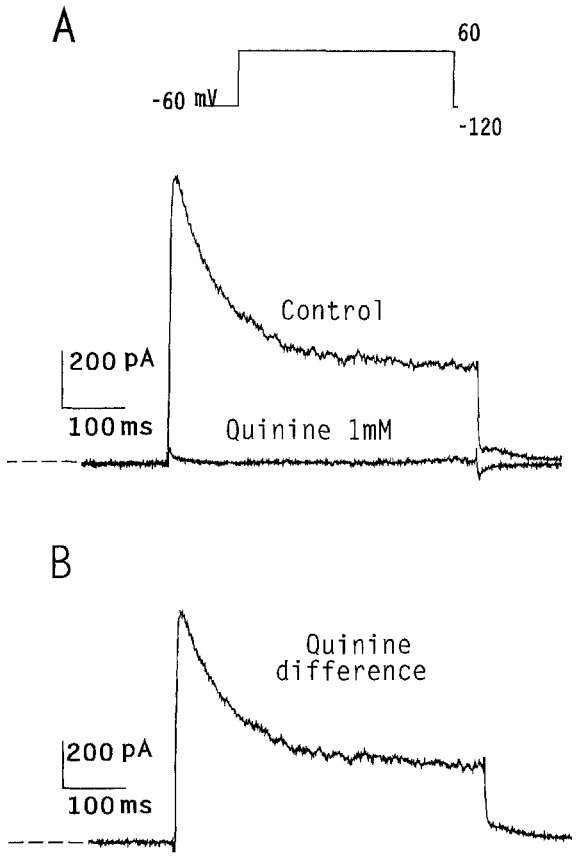

Fig. 8. Quinine blocks the fast-inactivating outward current. (*A*) Same cell as shown in Fig. 7. The cell was held at −60 mV and stepped to +60 mV for 500 msec. A pronounced time-dependent outward current is apparent. The trace labeled "*Quinine 1 mM*" was obtained 30 sec after application of quinine from a pipette located ≈100 μm from the cell. (*B*) The quinine difference current, obtained by subtracting current recorded after quinine application from control current.

10*C*. This cell exhibited little outward current at depolarized potentials. Inward current activated at hyperpolarized potentials was abolished (> 90% block) by 5 mM externally applied Cs^+, leaving only a linear "leak" current (2.5 GΩ) at negative potentials. Similar results were observed in three other cells with Cs^+ reducing the inward current at −120 mV by 93 ± 3%.

Time-dependent Decay of the Inward Rectifier at Negative Potentials

Time-dependent decay of the inward current at hyperpolarized potentials is characteristic of the inward rectifier in several different cell types. This reduction of the inward current at negative potentials is attributable, in part, to blockage by external Na^+ (Ohmori, 1978; Lindau & Fernandez, 1986; Gallin & McKinney, 1988*b*; Adams & Nonner, 1990; Kelly et al., 1992). In rabbit RPE cells, I_{KI} also exhibits a time-dependent decay at potentials hyperpolarized to −100 mV. We tested whether the decay of the inward rectifier arose from blockage by external Na^+, by recording I_{KI} in standard external Ringer solution and then in Na^+-free solution (substituting $NMDG^+$ for Na^+) (Fig. 11). In standard external Ringer solution, time-dependent decay of the inwardly rectifying current was readily observed at −160 mV (Fig. 11*A*). When external Na^+ was replaced by $NMDG^+$, the decay of the steady-state inward current at negative potentials was largely removed (Fig. 11*B*). Similar results were found in three other cells.

Effect of K^+ and Na^+ Replacement in Rabbit RPE Cells

When K^+ ions were replaced with TEA^+ in the external Ringer and 140 mM CsCl in the recording electrode, inward and outward voltage-dependent currents were no longer apparent and current-voltage plots revealed only a time-independent leakage current of 2-3 GΩ (n = 3, *not shown*), confirming that the membrane of rabbit RPE cells is dominated by K^+ conductances. In addition, we studied a further 25 cells using standard whole-cell recording and three cells using perforated-patch recording methods, with both external Na^+ and K^+ ions replaced with $NMDG^+$ and 140 mM CsCl in the electrode. In none of the cells recorded from in K^+ and Na^+-free Ringer did we observe depolarization-activated Ca^{2+} current. However, in some cells, in the absence of K^+ and Na^+, we observed a current which developed with time during recording, showed weak outward rectification and reversed around 0 mV. Further studies are currently underway to investigate the ionic dependence and regulation of this current, and these will be described elsewhere.

Discussion

In the present study, we have used patch clamp recording to examine membrane properties and whole-cell K^+ currents in cultured rabbit RPE cells. Cultured rabbit RPE cells express at least three voltage-dependent K^+ currents; two outwardly rectifying K^+ currents and an inwardly rectifying K^+ current are described. Details of these currents are discussed below and compared to K^+ currents described for RPE cells from other species as well as in other cell types. This report extends previous ion transport studies in the rabbit retinal pigment epithelium (Frambach, Valentine & Weiter, 1988) by providing the first account of ionic currents at the whole-cell level. We also report that, using standard whole-cell recording conditions as well as perforated-patch

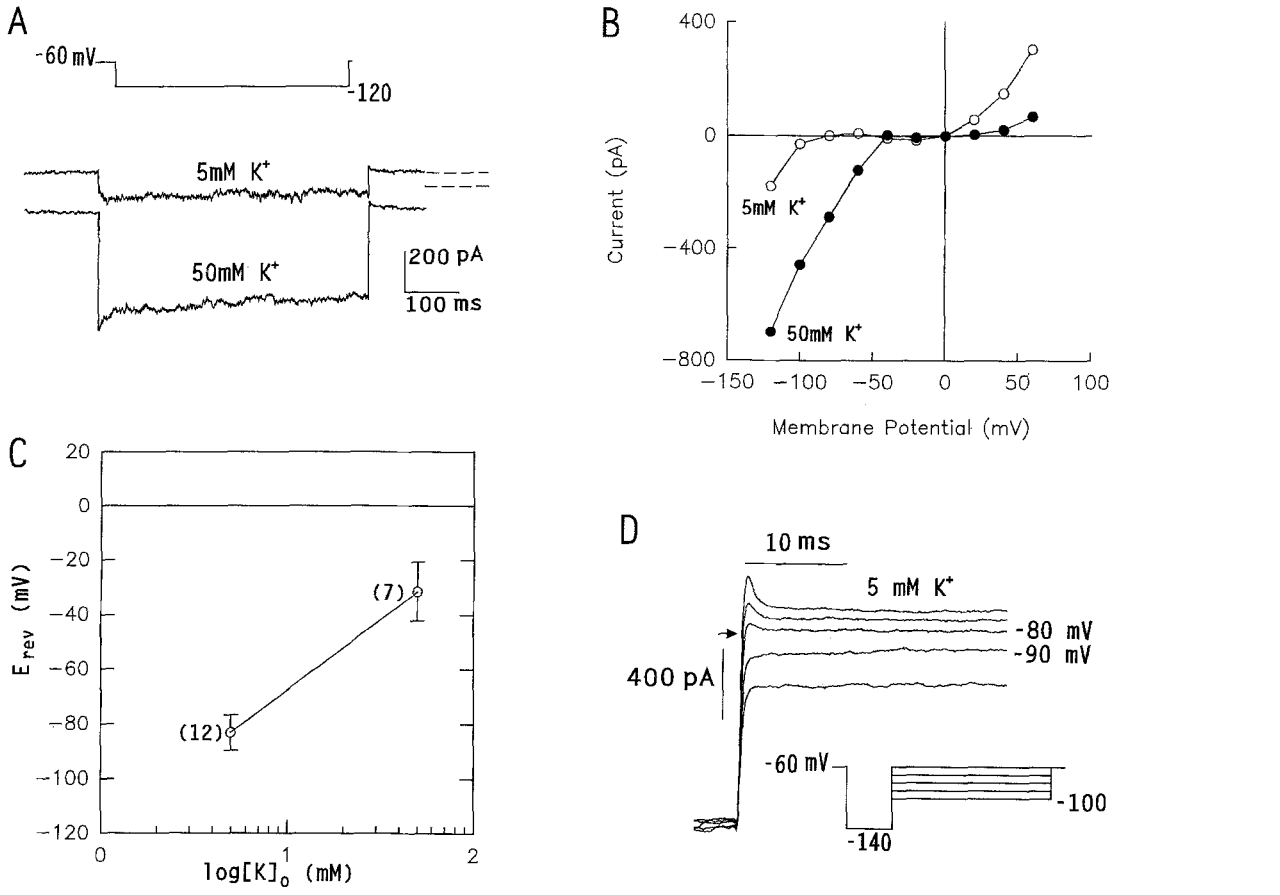

Fig. 9. The inwardly rectifying current in rabbit RPE cells is dependent on $[K^+]_o$. (*A*) Inward current was activated by stepping the membrane potential from a holding potential of −60 to −120 mV for 500 msec. The cell was superfused with standard 5 K^+ Ringer and then subsequently with 50 mM K^+ Ringer. (*B*) *I-V* relationship for the cell shown in *A*. Increasing external K^+ from 5 mM K^+ (○) to 50 mM K^+ (●), shifted the reversal potential and the voltage at which the rectification occurred, positive along the voltage axis. (*C*) Zero current potentials (V_{rev}) for 7–12 cells are plotted as a function of $[K^+]_o$. The straight line is the least squares best fit of the data, with a slope of 50 mV per 10-fold change of $[K^+]_o$. The number of cells studied at each $[K^+]_o$ is indicated in parentheses beside each data point. (*D*) Time-dependent decay of the inward K^+ current for another cell, bathed in 5 mM $[K^+]_o$. From a holding potential of −60 mV, the membrane potential was stepped to −140 mV to activate inwardly rectifying K^+ current and then to various potentials, as indicated by the voltage command protocol. Tail currents reversed direction at ≈−82 mV, as indicated by the arrow, which is close to the predicted equilibrium potential for K^+. Cell capacitance was 22 pF for the cell in panels *A* and *B* and 32 pF for the cell in panel *D*.

methods, we were unable to find evidence for voltage-dependent Na^+ or Ca^{2+} currents in rabbit RPE cells.

Voltage-dependent K^+ Currents in RPE Cells: Comparison with Other Cell Types

The predominant current expressed in 91% of rabbit RPE cells is an outwardly rectifying current, I_K, which activated with a slight delay at potentials positive to −40 mV and decayed slowly after reaching a peak. The outward current described in rabbit RPE cells is selective for K^+; tail currents reversed direction at −73 mV and the reversal potential shifted 50 mV per 10-fold change in $[K^+]_o$, as expected for a K^+-dependent current. Since tail currents were well described by a single exponential, with similar time constants in different $[K^+]_o$, this further suggests that the outwardly rectifying K^+ current is the dominant outward current expressed in rabbit RPE cells. Outward current in rabbit RPE cells was further characterized using pharmacological blockers of voltage-dependent K^+ currents. Extracellular TEA and Ba^{2+}, which have been shown to block the delayed rectifier K^+ currents in a variety of cell types including human (Strauß et al., 1993; Wen et al., 1993), monkey (Wen et al., 1993), frog (Hughes & Steinberg, 1990) and turtle (Fox & Steinberg, 1992) RPE cells, reversibly decreased outward K^+ current in rabbit RPE cells. Low concentrations of 4-AP (0.1–1 mM) also reduced the outward current; however, the

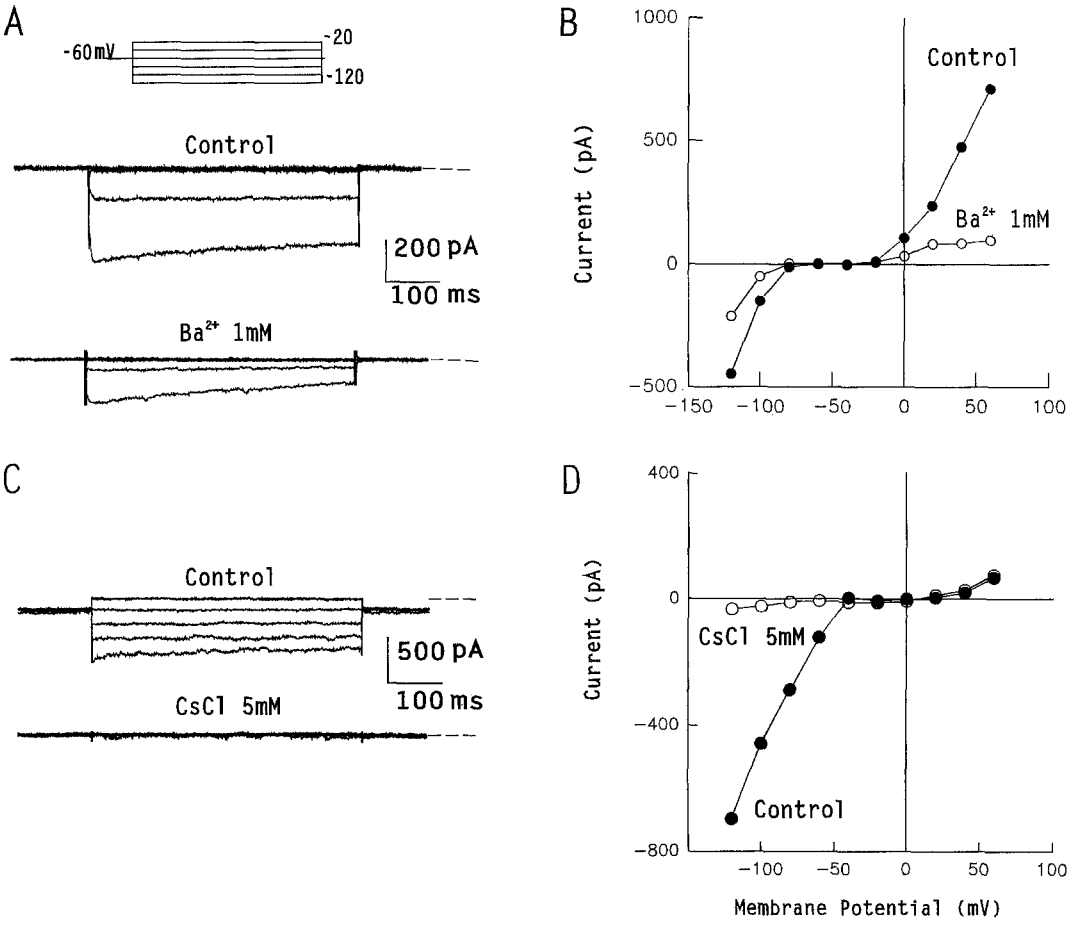

Fig. 10. Inwardly rectifying K^+ current is blocked by Ba^{2+} and Cs^+. (*A*) The cell is held at a holding potential of −60 mV and stepped from −120 to +60 mV in 20 mV increments. The top panel shows currents recorded at potentials from −120 to −20 mV in standard 5 mM K^+ Ringer. The bottom panel shows currents recorded from the same cell following a 30 sec application of 1 mM external Ba^{2+} via an application pipette. Currents were subtracted for a linear leak of 1 GΩ. (*B*) *I-V* plot for the cell in *A*, before (●) and during Ba^{2+} application (○). Current values were measured 10 msec after the onset of the voltage pulses from −120 to +60 mV. Ba^{2+} reduces both inward and outward current in this cell. (*C*) Currents recorded from another cell bathed in 50 mM $[K^+]_o$, before (●) and after (○) the addition of 5 mM Cs^+ via an application pipette. (*D*) *I-V* plot for the cell shown in *C*. The cell shows pronounced inward current at negative potentials which was abolished by exposure to Cs^+. Capacitance of the cells shown was 37 pF for the cell in *A* and *B* and 22 pF for the cell in *C* and *D*.

block with 1 mM 4-AP was only partially reversible. The outward K^+ current described here in rabbit RPE cells shows a similar pharmacological specificity to the outward K^+ current described in frog RPE cells, where outward K^+ current was also sensitive to block by low concentrations of 4-AP as well as by TEA and Ba^{2+} (Hughes & Steinberg, 1990).

The voltage dependence and kinetics of the outwardly rectifying K^+ current, I_K, in rabbit RPE cells resembles the delayed rectifier K^+ current described in several other nonexcitable cells, such as T lymphocytes (Cahalan et al., 1985; DeCoursey et al., 1987) and macrophages (Ypey & Clapham, 1984) as well as in isolated RPE cells from frog (Hughes & Steinberg, 1990). Like frog RPE cells, outward K^+ current in rabbit RPE cells activated following a brief delay at potentials positive to −40 mV, exhibited slow time-dependent decay at positive potentials and was inactivated by depolarizing potentials of −30 mV or more positive. Delayed rectifier K^+ current has also been described in whole-cell measurements of cultured human and monkey RPE cells but, although the delayed rectifier in primate RPE cells activated over a similar voltage range to I_K in rabbit RPE cells, the delayed outward rectifier in primate RPE cells was virtually noninactivating (Wen et al., 1993).

In a very small number of cultured rabbit RPE cells (3–4%), we observed a fast-inactivating outward K^+ current, I_{Kt}. In rabbit RPE cells, I_{Kt} activated around −50 mV or more negative and inactivated rapidly at depolarized potentials. Inactivation time constants for I_{Kt}, at depolarized potentials, were 10-fold faster than time constants measured for the delayed rectifier current I_K. However, the extremely small number of cells in

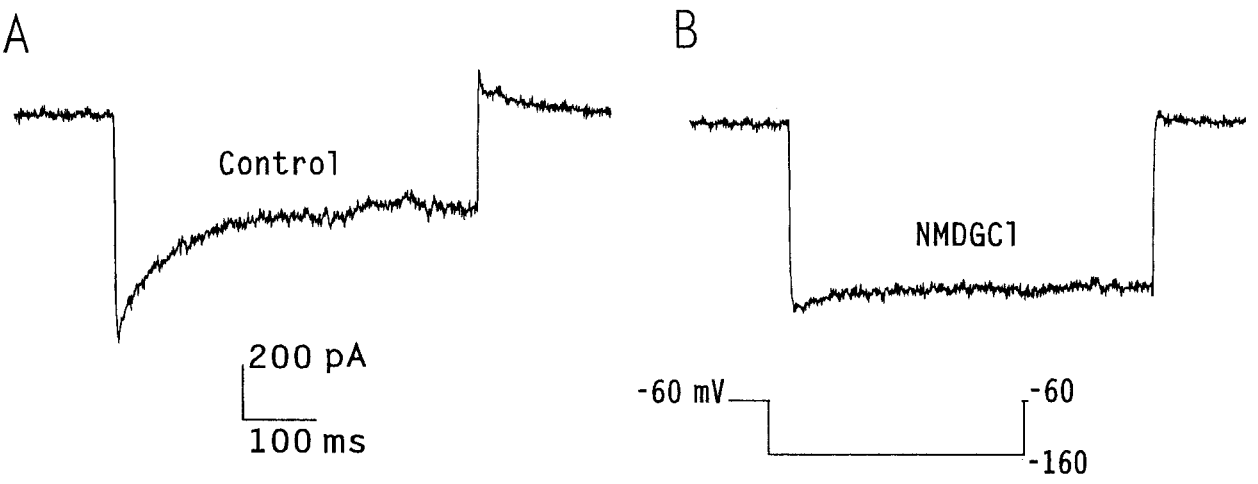

Fig. 11. Na^+-dependent reduction of the inward current at negative potentials. (*A*) Whole-cell current recorded from a cell bathed in standard 5 mM K^+ Ringer (Na^+ containing). Cell was held at −60 mV and stepped to −160 mV. (*B*) Inward current recorded from the same cell in Na^+-free ($NMDG^+$) external solution. Time-dependent decay of the inward current has been largely removed in nominally Na^+-free bathing solution. Capacitance of the cell was 41.5 pF.

which the fast-inactivating current was found has precluded extensive characterization of the properties and conditions regulating I_{Kt}. The fast-inactivating outward K^+ current in rabbit RPE cells resembles the inactivating delayed rectifier K^+ current, I_{nK}, described in T lymphocytes (Cahalan et al., 1985; Lewis & Cahalan, 1988), macrophages (Ypey & Clapham, 1984) and more recently in porcine granulosa cells (Mattoli, Barboni & DeFelice, 1993). In addition, an inactivating outward K^+ current, with a threshold for activation at potentials negative to −40 mV, has also been described in turtle RPE cells (Fox & Steinberg, 1992). Like I_{Kt} in rabbit RPE cells, which was completely blocked by quinine, the time- and voltage-dependent outward current in turtle RPE cells was abolished (>80% block) by quinidine, the D-stereoisomer of quinine.

In 41% of rabbit RPE cells, an inwardly rectifying current was activated at hyperpolarized potentials. The inwardly rectifying current was shown to be carried by K^+ ions based on experiments examining voltage dependence, ionic selectivity and pharmacological blockage of the inward current. The inward current was dependent on $[K^+]_o$, with the zero current potential shifting positive as $[K^+]_o$ was increased. Examination of the time- and voltage-dependent decay of the inward current confirmed that current relaxations reversed direction close to E_K. The presence of these relaxations demonstrates that time-dependent gating of K^+ channels contributes to inward rectification. The inward rectifier in rabbit RPE cells was blocked by both Ba^{2+} and Cs^+, which have been shown to block inward rectifiers in a number of different cell types (Standen & Stanfield, 1978; Gallin & McKinney, 1988*b*; Cooper et al., 1990; Cooper, Rae & Dewey, 1991; Kelly et al., 1992; Ishikawa & Cook, 1993), including frog (Hughes & Steinberg, 1990), cultured human (Strauß et al., 1993; Wen et al., 1993) and monkey (Wen et al., 1993) RPE cells.

At hyperpolarized potentials, rabbit RPE cells exhibited a time-dependent decay of steady-state inward current, which was largely removed when external Na^+ was replaced with $NMDG^+$. Na^+-dependent reduction of the inward current at hyperpolarized potentials is also a characteristic of the inward rectifier in frog skeletal muscle (Standen & Stanfield, 1978), macrophages (Gallin & McKinney, 1988*b*), osteoclasts (Kelly et al., 1992) and mammalian lens epithelial cells (Cooper et al., 1991) and has been attributed to low-affinity block of the K^+ channel by Na^+ ions. The inwardly rectifying K^+ current in cultured human and monkey RPE cells also exhibits Na^+-dependent reduction at potentials negative to −120 mV, although Na^+-dependent inactivation was not observed in fresh primate cells (Wen et al., 1993).

The macroscopic inwardly rectifying K^+ current in rabbit RPE cells shows similarities to the inward rectifier described in cultured primate RPE cells (Wen et al., 1993). Like the inward rectifier in primate RPE cells, the inward rectifier in rabbit RPE cells exhibited pronounced rectification at depolarized potentials, with less than 20% of the maximum conductance still active around E_K (≈45 pS/pF), and a strong dependence on extracellular $[K^+]_o$. In rabbit RPE cells, increases in $[K^+]_o$ enhanced the inward K^+ conductance and shifted both the zero current potential and the voltage around which the current rectifies in the positive direction. In contrast, the inward rectifier in frog RPE cells decreases more gradually at depolarizing voltages and the conductance does not increase with increasing $[K^+]_o$, although the reversal potential of the inward current in frog RPE cells is dependent on $[K^+]_o$.

Other Currents in Rabbit RPE Cells

The rabbit RPE cell membrane is dominated by K^+ conductances. We found no evidence for voltage-dependent Na^+ or Ca^{2+} currents using either standard whole-cell or perforated-patch recording, even under conditions which favored their identification such as with K^+ currents blocked or following K^+ and Na^+ ion substitution. Although we did not observe depolarization-activated Ca^{2+} current, it is possible that in cultured rabbit RPE cells, Ca^{2+} channels are expressed at a very low density and may not be observed using standard calcium concentrations. Voltage-dependent Ca^{2+} channels have been reported in rat RPE cells, where they appear to be similar to the L-type calcium channels described in neurons and cardiac cells (Ueda & Steinberg, 1993).

Function of Voltage-dependent K^+ Conductances in Retinal Pigment Epithelial Cells

The expression of individual K^+ channel types in cultured rabbit RPE cells showed considerable heterogeneity with only 37% of studied cells expressing both inward and outward currents. Since rabbit RPE cells at 2–5 days in culture are beginning to proliferate, it is possible that cell differentiation may contribute to the heterogenous distribution of ion channels observed in these cells. Heterogeneity in the expression of K^+ conductances has also been reported for cultured human RPE cells, with only 25% of cells recorded from exhibiting both inward and outward K^+ conductances (Strauß et al., 1993). However, even in freshly isolated frog RPE cells only a portion of the cell population was found to express an inward rectifier and in those cells the expression of inward K^+ current was correlated with membrane potentials of -50 mV or greater (Hughes & Steinberg, 1990).

In cultured rabbit RPE cells, we found no clear correlation between membrane potential and the expression of either outward or inward K^+ currents. Recordings made from cells cultured for 24 hr in culture or between 2–5 days in culture showed a similar heterogenous distribution of K^+ currents. With regard to the appearance of rapidly inactivating K^+ current (I_{Kt}) in 3–4% of rabbit RPE cells, it is possible that the infrequent appearance of this current may be the result of cell differentiation in culture since this current was never observed in cells cultured for less than three days. In other nonexcitable cells a direct link has been established between the expression of inactivating delayed rectifier current and cell proliferation (Chandry et al., 1986; Konishi, 1989; Mattioli et al., 1993). In addition, a recent study examining whole-cell currents from both freshly isolated and cultured fetal and adult human RPE cells has demonstrated that a transient A-type K^+ current is expressed in fetal RPE cells and in 33% of cultured adult human RPE cells (Wen et al., 1993). A-current was never observed in freshly isolated adult human RPE cells. Based on these observations, the authors suggested that ion channels may be developmentally regulated in mammalian RPE cells and that dedifferentiation to a more immature phenotype may occur when adult RPE cells are maintained in culture.

Alterations in subretinal $[K^+]$ are known to occur following light-dark induced changes in photoreceptor activity and are accompanied by corresponding alterations in transepithelial potential (Steinberg & Miller, 1979; Steinberg et al., 1980; Oakley & Steinberg, 1982; Immel & Steinberg, 1986; La Cour et al., 1986). Experiments conducted using isolated RPE-choroid preparations from several vertebrate species, including rabbit, have identified several different active and passive transport mechanisms at the RPE apical and basal membranes (Frambach et al., 1988; Joseph & Miller, 1991). These include an apical ouabain-sensitive Na^+-K^+ pump and both apical and basal Ba^{2+}-sensitive K^+ conductances.

The voltage-dependent K^+ conductances described here, in cultured rabbit RPE cells, could provide conductive pathways to support electrogenic pump activity and contribute to $[K^+]$ homeostasis in the subretinal space. Decreases in subretinal $[K^+]$, following light activation of photoreceptors, transiently hyperpolarizes the RPE apical membrane and inhibits the Na^+-K^+ pump (Joseph & Miller, 1991). Activation of the inward rectifier K^+ current during this process would limit this hyperpolarization by clamping the membrane potential around E_K and increasing K^+ efflux to the subretinal space. Subsequent increases in subretinal $[K^+]$ and the resulting membrane depolarization would tend to decrease the inwardly rectifying K^+ conductance, thus minimizing K^+ efflux through this pathway and enhancing electrogenic K^+ transport into the cell.

The outwardly rectifying K^+ conductance in rabbit RPE cells may provide an efflux pathway for K^+ which enters the cell via electrogenic K^+ transport. However, since the activation threshold for I_K, the predominant outward K^+ conductance in rabbit RPE cells, was close to the resting potential measured for these cells in culture, and considerably depolarized with respect to values measured for the membrane potential of the intact epithelium in several species (Miller & Steinberg, 1977; Steinberg, Miller & Stern, 1978; Joseph & Miller, 1991), it is unlikely that this current would contribute significantly to the establishment of the resting membrane potential. Phagocytosis of shed photoreceptor outer segments is one of the major roles of RPE cells, which carry out a diverse array of functions to maintain and support the viability of retinal photoreceptors (Steinberg & Miller, 1979). Activation of outwardly rectify-

ing K^+ conductances has been demonstrated to accompany the membrane potential changes associated with phagocytosis of particles by macrophages (Ince et al., 1988). Thus, it is possible that, in addition to ion transport, K^+ channels may be involved in the phagocytotic action of the RPE cells and may contribute to other cellular functions concerned with the maintenance of photoreceptor cell viability.

We wish to thank Jonathan Blay for his advice on matters related to cell culture, John Poyer and Susan Howlett for their comments on the manuscript and Christine Jollimore for her expert technical support. This work was funded by Natural Sciences and Engineering Research Council of Canada grant OGP0121657 and the Retinitis Pigmentosa Research Foundation. Q-P.T. is funded by an Retinitis Pigmentosa Research Foundation Studentship award.

References

Adams, D.J., Nonner, W. 1990. Voltage-dependent potassium channels: gating, ion permeation and block. *In:* Potassium channels: structure, classification, function and therapeutic potential. N.S. Cook, editor, pp 23–60. Ellis Horwood, Chichester, UK

Armstrong, C.M., Taylor, S.R. 1980. Interaction of barium ions with potassium channels in squid giant axons. *Biophys. J.* **30:**473–88

Bird, A.C. 1989. Pathogenesis of serous detachment of the retina and pigment epithelium. *In:* Retina, vol. 2. B.M. Glaser and R.G. Michels, editors. pp. 99–105. C.V. Mosby, St. Louis, MO

Cahalan, M.D., Chandy, K.G., Decoursey, T.E., Gupta, S. 1985. A voltage-grated K^+ channel in human T lymphocytes. *J. Physiol.* **358:**197–237

Chandry, K.G., Decoursey, T.E., Fischbach, M., Cahalan, M.D., Gupta, S. 1986. An altered K^+ channel expression in abnormal T lymphocytes from mice with the LPr gene mutation. *Science* **233:** 1197–1200

Cooper, K., Rae, J.L., Gates, P., Dewey, J. 1990. Electrophysiology of cultured human lens epithelial cells. *J. Membrane Biol.* **117:** 285–298

Cooper, K., Rae, J.L., Dewey, J. 1991. Inwardly rectifying potassium current in mammalian lens epithelial cells. *Am. J. Physiol.* **261:** C115–C123

Decoursey, T.E., Chandy, K.G., Gupta, S., Cahalan, M.D. 1987. Two types of potassium channels in murine T Lymphocytes. *J. Gen. Physiol.* **89:**379–404

Fox, J.A., Pfeffer, B., Fain, G. 1988. Single-channel recordings from cultured human retinal pigment epithelium. *J. Gen. Physiol.* **91:** 193–222

Fox, J.A., Steinberg, R.H. 1992. Voltage-dependent currents in isolated cells of the turtle retinal pigment epithelium. *Pfluegers Arch.* **420:**451–460

Frambach, D.A., Valentine, J.L., Weiter, J.J. 1988. Modulation of rabbit retinal pigment electrogenic transport by alpha-1 adrenergic stimulation. *Invest. Ophthalmol. Vis. Sci.* **29:**814–817

Gallin, E.K., McKinney, L.C. 1988*a*. Inwardly rectifying whole-cell and single-channel K currents in the murine macrophage cell line J774.1. *J. Membrane Biol.* **103:**41–53

Gallin, E.K., McKinney, L.C. 1988*b*. Patch-clamp studies in human macrophages: Single channel and whole-cell characterization of two K^+ conductances. *J. Membrane Biol.* **103:**55–66

Hamill, O.P., Marty, A., Neher, E., Sakmann, B., Sigworth, F.J. 1981. Improved patch-clamp techniques for high-resolution current recording from cells and cell-free membrane patches. *Pfluegers Arch.* **391:**85–100

Horn, R., Marty, A. 1988. Muscarinic activation of ionic currents measured by a new whole-cell recording method. *J. Gen. Physiol.* **92:** 145–159

Hughes, B.A., Botchkin, L.M., Steinberg, R.H. 1990. Whole-cell currents in isolated retinal pigment epithelial (RPE) cells of the normal pigmented rat. *Invest. Ophthalmol. Vis. Sci.* **31(suppl):**177

Hughes, B.A., Steinberg, R.H. 1990. Voltage-dependent currents in isolated cells of the frog retinal pigment epithelium. *J. Physiol.* **428:**273–297

Immel, J., Steinberg, R.H. 1986. Spatial buffering of K^+ by the retinal pigment epithelium. *J. Neurosci.* **6:**3197–3204

Ince, C., Coremans, J.M.C.C., Ypey, D.L., Leijh, P.C.J., Verveen, A.A., Van Furth, R. 1988. Phagocytosis by human macrophages is accompanied by changes in ionic channel currents. *J. Cell Biol.* **106:**1873–1878

Ishikawa, T., Cook, D.I. 1993. Effects of K^+ channel blockers on inwardly and outwardly rectifying whole-cell K^+ currents in sheep parotid secretory cells. *J. Membrane Biol.* **133:**29–41

Joseph, D.P., Miller, S.S. 1991. Apical and basal membrane ion transport mechanisms in bovine retinal pigment epithelium. *J. Physiol.* **435:**439–463

Kelly, M.E.M., Dixon, S.J., Sim, S.M. 1992. Inwardly rectifying potassium current in rabbit osteroclast: A whole-cell and single-channel study. *J. Membrane Biol.* **126:**171–181

Konishi, T. 1989. Voltage-dependent K^+ channels in mouse Schwann cells. *J. Physiol.* **411:**115–130

La Cour, M., Lund-Anderson, H., Zeuthen, T. 1986. Potassium transport of the frog retinal pigment: autoregulation of potassium activity in the subretinal space. *J. Physiol.* **375:**461–479

Lewis, R.S., Cahalan, M.D. 1988. Subset-specific expression of potassium channels in developing murine T lymphocytes. *Science* **239:** 771–775

Lindau, M., Fernandez, J.M. 1986. A patch-clamp study of histamine-secreting cells. *J. Gen. Physiol.* **88:**349–368

Marmor, M.F. 1989. Mechanisms of normal retinal adhesion. *In:* Retina, vol. 3. B.M. Glaser, R.G. Michels, editors. pp. 71–88. C.V. Mosby, St. Louis, MO

Mattoli, M., Barboni, B., DeFelice, L.J. 1993. Calcium and potassium currents in porcine granulosa cells maintained in follicular or monolayer tissue culture. *J. Membrane Biol.* **134:**75–83

Miller, S.S., Steinberg, R.H. 1977. Passive ionic properties of frog retinal pigment epithelium. *J. Membrane Biol.* **36:**337–372

Miller, S.S., Steinberg, R.H. 1982. Potassium transport across the frog retinal pigment epithelium. *J. Membrane Biol.* **67:**199–209

Oakley, B.H. 1977. Potassium and the photoreceptor dependent pigment epithelial hyperpolarization. *J. Gen. Physiol.* **70:**405–424

Oakley, B.H., Green, D.G. 1976. Correlation of light-induced changes in retinal extracellular potassium concentration with the c-wave of the electroretinogram. *J. Neurophysiol.* **39:**1117–1133

Oakley, B.H., Steinberg, R.H. 1982. Effects of maintained illumination upon $[K^+]_o$ in the subretinal space of the frog retina. *Vision Res.* **22:**767–773

Ohmori, H. 1978. Inactivation and steady-state current noise in the anomalous rectifier of tunicate egg cell membrane. *J. Physiol.* **281:** 77–99

Quinn, R.H., Miller, S.S. 1992. Ion transport mechanisms in native human retinal pigment epithelium. *Invest. Ophthalmol. Vis. Sci.* **33:**3513–3527

Sakmann, B., Trube, G. 1984. Conductance properties of single inwardly rectifying potassium channels in ventricular cells from guinea-pig heart. *J. Physiol.* **347:**641–657

Standen, N.B., Stanfield, P.R. 1978. A potential- and time-dependent

blockage of inward rectification in frog skeletal muscle fibres by barium and strontium ions. *J. Physiol.* **280:**169–191

Stanfield, P.R. 1983. Tetraethylammonium ions and the potassium permeability of excitable cells. *Rev. Physiol. Biochem. Pharmacol.* **97:**1–67

Steinberg, R.H., Miller, S.S. 1979. Transport and membrane properties of the retinal pigment epithelium. *In:* The Retinal Pigment Epithelium. K.M. Zinn, M.F. Marmor, editors. pp. 205–225. Harvard University, Cambridge, MA

Steinberg, R.H., Miller, S.S., Stern, W.H. 1978. Initial observations on the isolated retinal pigment epithelium-choroid of the cat. *Invest. Ophthalmol. Vis. Sci.* **17:**675–678

Steinberg, R.H., Oakley, B.H., Neimeyer, G. 1980. Light-evoked changes in $[K^+]_o$ in retina of the intact cat eye. *J. Neurosci.* **44:** 897–921

Strauß, O., Weinrich, M. 1992. Retinal pigment epithelial cells from the rat in culture: Whole-cell recordings of membrane currents. *Invest. Ophthalmol. Vis. Sci.* **33(suppl):**1103

Strauß, O., Richard, G., Weinrich, M. 1993. Voltage-dependent potassium currents in cultured human retinal pigment epithelial cells. *Biochem. Biophys. Res. Commun.* **191:**775–781

Tao, Q.-P., Kelly, M.E.M., Rafuse, P.E. 1993. Potassium and anion currents in rabbit retinal pigment epithelial cells. *Invest. Opthalmol. Vis. Sci.* **34(suppl.):**857

Ueda, Y., Steinberg, R.H. 1993. Voltage-operated calcium channels in fresh and cultured rat retinal pigment epithelial cells. *Invest. Ophthalmol. Vis. Sci.* **34:**3408–3418

Wen, R., Lui, G.M., Steinberg, R.H. 1993. Whole-cell K^+ currents in fresh and cultured cells of the human and monkey retinal pigment epithelium. *J. Physiol.* **465:**121–147

Ypey, D.L., Clapham, D.E. 1984. Development of a delayed outward-rectifying K^+ conductance in cultured mouse peritoneal macrophages. *Proc. Natl. Acad. Sci. USA* **81:**3083–3087

Zauberman, H. 1979. Adhesive forces between the retinal pigment epithelium and sensory retina. *In:* The Retinal Pigment Epithelium. K.M. Zinn, M.F. Marmor, editors. pp. 192–202. Harvard University, Cambridge, MA

Zinn, K.M., Benjamin-Henkind, J.V. 1979. Anatomy of the human retinal pigment epithelium. *In:* The Retinal Pigment Epithelium. K.M. Zinn, M.F. Marmor, editors. pp. 3–27. Harvard University, Cambridge, MA